J. Fluid Mech. (2009), *vol.* 641, *pp.* 195–204.
doi:10.1017/S0022112009992229

The spreading phase in Lighthill's model of the Weis-Fogh lift mechanism

DARREN CROWDY†

Department of Mathematics, Imperial College London, 180 Queen's Gate, London, SW7 2AZ, UK

(Received 12 February 2009; revised 31 August 2009; accepted 11 September 2009; first published online 23 November 2009)

Lighthill's analysis (*J. Fluid Mech.*, vol. 60, 1973, p. 1) of the Weis-Fogh lift mechanism is extended to include the spreading phase of the cycle. Lighthill proposed a two-dimensional inviscid irrotational analytical model to compute the circulation around two flat plates (the wings) as they open out, in opposite directions, about a common centre of rotation taken to be at the point of contact of an edge of each plate (the 'opening phase'). At a critical opening angle, the plates separate and move apart horizontally (the 'spreading phase'). During this second phase, the fluid region becomes doubly connected and is not analysed by Lighthill. It can, however, also be studied analytically and the results are presented here. We also extend a similar analysis, in an application to turbomachinery, due to Furber & Ffowcs Williams (*J. Fluid Mech.*, vol. 94, 1979, p. 519).

1. Introduction

In a paper in this journal in Lighthill (1973) gave the first mathematical rationalization of a newly discovered lift mechanism reported in the same year by Weis-Fogh (1973). It was observed in a study of the hovering motions of the chalcid wasp known as *Encarsia formosa* (Acheson 1992). It is a novel mechanism that does not rely on vortex shedding for the generation of lift; rather, its success rests on the instantaneous generation of net circulation around two wings brought about by a change of flow domain topology as the wings carry out their flapping protocol.

Lighthill (1973) explained the mechanism by considering an inviscid, irrotational two-dimensional model. By means of a complex variable approach and a Schwarz–Christoffel mapping, he produced an explicit mathematical representation of the solution for the 'opening phase'. During this stage the two wings are initially close to parallel and are touching at their two lowest ends; they remain in contact but fan out, about a centre of rotation given by the point of contact of the lowest edges of the wings, until they reach a critical opening angle. At this instant, and as the wings are still fanning out, the wings detach (the 'spreading phase') and move apart along a horizontal axis. Lighthill's analysis, valid only during the opening phase, allows the calculation of the net circulation Γ around each wing at the instant of separation. For plates of length c opening up with constant angular velocity Ω to angle ϕ he found

$$\Gamma = \Omega c^2 g(\phi/2), \tag{1}$$

where the function $g(\alpha)$ is given as an integral of Schwarz–Christoffel type and is graphed in figure 4 of Lighthill (1973). Since, in ideal flow theory, a flow is

† Email address for correspondence: d.crowdy@imperial.ac.uk

determined by the instantaneous motion of the boundaries, it is not altogether clear how it can be justified that the circulation around the plates *after* separation is given by the circulation just *before* separation. However, in a closely related problem operating under the same principles, Furber & Ffowcs Williams (1979) investigate this matter and give more detailed explanations as to how and why the circulation around each wing even after separation can be expected to be given by Γ. In this article, we proceed under the assumption that the relevant Γ is indeed given by (1).

Edwards & Cheng (1982) later showed that $g(\alpha)$ has the explicit analytical form

$$g(\alpha) = \left(1 - \frac{2\alpha}{\pi}\right) \Big/ 2\sin(2\alpha) \left(\frac{\alpha}{\pi}\right)^{2\alpha/\pi} \left(1 - \frac{\alpha}{\pi}\right)^{2-2\alpha/\pi}. \tag{2}$$

Motivated by evidence presented by Maxworthy (1979) suggesting that the production of shed vorticity at the leading edge of the wings plays a significant (if not dominant) role in the mechanism, they also included the effect of this vorticity using a single-vortex shedding model. Referring to Lighthill's determination of the circulation Γ at the end of the opening phase, Edwards & Cheng (1982) state: 'its significance lies entirely on the influence of this Γ on the subsequent *lift development* during the spreading phase, which is not determined by the initial Joukowski lift $\rho U \Gamma$ alone. . . . Of no less importance is the evaluation of the force experienced by, as well as moment and power required of, an insect during the open phase of this model.' Lighthill does not calculate this lift development: there are mathematical difficulties due to the change in topology of the fluid domain (it becomes doubly connected). Since Lighthill's early theoretical work, there have been a variety of other experimental (e.g. Spedding & Maxworthy 1986) and numerical (e.g. Mao & Xin 2003) investigations of the Weis-Fogh mechanism in which additional physical effects have been incorporated.

Notwithstanding that other physical effects play important roles in the Weis-Fogh mechanism, this paper makes a theoretical contribution to the topic by completing the analysis of Lighthill's original model. Our principal objective here is to demonstrate the use of a new calculus, described by Crowdy (2009), applicable to the study of ideal flows in multiply connected domains. The Weis-Fogh problem presents a paradigmatic physically motivated example of a flow involving a change in topology and, until now, only the simply connected stage of an idealized model of the process has been analysed in the literature: here we complete the picture by analysing the doubly connected stage under the same model assumptions as those of Lighthill. Another case in point is the related work of Furber & Ffowcs Williams (1979), who explored engineering applications of the Weis-Fogh mechanism in the design of an axial-flow compressor. They also present a model of the relevant process but only consider the simply connected stage: in § 6 we also complete their analysis and derive analogous solutions to the doubly connected phase of that model.

2. Mathematical formulation

Following Lighthill (1973), consider irrotational motion in a fluid of uniform density $\hat{\rho} = 1$. Each wing is modelled as a flat plate with unit length (so $c = 1$) and we let $\Omega = 1$ during the opening phase. Let ϕ be the critical opening angle at which the plates separate with equal and opposite speed $U(t)$ (henceforth U, although it is understood to be time dependent). We focus on the case $\phi = 2\pi/3$ and assume that there are circulations $\pm\Gamma$ as calculated by Lighthill (1973) around each wing so that, for $\phi = 2\pi/3$, then $\Gamma = 0.69$. Note that U can be arbitrarily specified in our model

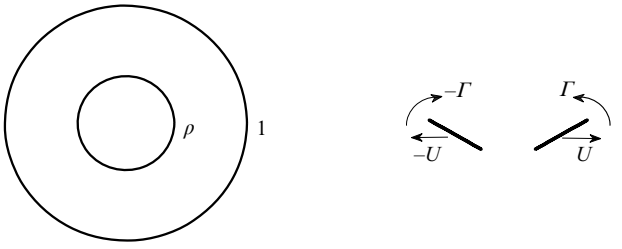

FIGURE 1. Schematic showing a typical image, for $\phi = 2\pi/3$, of $\rho(t) < |\zeta| < 1$ under the mapping $z(\zeta, t)$ in (4). Here, $|\zeta| = 1$ maps to the left wing.

but we later describe one prescription for determining it based on the assumptions that the circulations $\pm\Gamma$ around the wings are constant in time and that Kutta conditions are satisfied at the trailing edges of the wings after separation. There is still a singularity in the velocity field at the leading edge of each plate which, in reality, would result in vortex shedding there but this is ignored here. If a single plate is in isolation, a routine calculation using a Joukowski mapping from a unit disk to a unit-length plate inclined at an angle $(\pi + \phi)/2$ to the positive real axis (this is true of the leftmost plate) can be used to deduce that the Kutta condition at the trailing edge implies the following relationship between Γ and U:

$$U\pi\cos(\phi/2) = \Gamma. \tag{3}$$

This simple relation is expected to be modified by unsteady interaction effects between the two separating wings.

3. Conformal mapping

The flow exterior to the two wings after separation is doubly connected. At each instant there exists a conformal map, $z(\zeta, t)$ say, from some annulus $0 < \rho(t) < |\zeta| < 1$ in a parametric ζ-plane to the fluid region. Let the complex potential for the flow at each instant be $w(z, t)$. Given $z(\zeta, t)$, define $W(\zeta, t) \equiv w(z(\zeta, t), t)$. The problem is solved if both $z(\zeta, t)$ and $W(\zeta, t)$ can be found explicitly.

We have found that a formula for the conformal mapping to the fluid region exterior to the wings at any instant after they have separated is

$$z(\zeta, t) = \mathrm{i}A(t)\mathrm{e}^{-\mathrm{i}\phi/2}\left(\frac{P(\zeta\sqrt{\rho(t)}^{-1}\mathrm{e}^{\mathrm{i}\phi}, \rho(t))P(\zeta\sqrt{\rho(t)}\mathrm{e}^{\mathrm{i}\phi}, \rho(t))}{P(\zeta\sqrt{\rho(t)}^{-1}, \rho)P(\zeta\sqrt{\rho(t)}, \rho(t))}\right) - \mathrm{i}\,\mathrm{d}(t), \tag{4}$$

where $A(t)$, $\rho(t)$ and $\mathrm{d}(t)$ are real functions of time and

$$P(\zeta, \rho) \equiv (1 - \zeta)\prod_{k=1}^{\infty}(1 - \rho^{2k}\zeta)(1 - \rho^{2k}\zeta^{-1}). \tag{5}$$

Figure 1 shows an example for a typical choice of parameters. Equation (4) has been derived using results on multiply connected conformal slit mappings given by Crowdy & Marshall (2006). Let $s(t)$ denote the x-position of the midpoint of the rightmost plate. Given $s(t)$, the parameters $A(t)$, $\rho(t)$ and $\mathrm{d}(t)$ can be found by imposing various geometrical requirements. Details are given in the Appendix.

4. The complex potential

By making use of a general calculus for planar ideal flows described by Crowdy (2009), the required instantaneous complex potential $W(\zeta, t)$ in the annulus $\rho(t) < |\zeta| < 1$ can also be found. It is

$$W(\zeta, t) = \Gamma G_0(\zeta, \sqrt{\rho(t)}) - \Gamma G_1(\zeta, \sqrt{\rho(t)}) + W_U(\zeta, t), \tag{6}$$

where

$$G_0(\zeta, \alpha) \equiv -\frac{\mathrm{i}}{2\pi} \log\left(\frac{|\alpha| P(\zeta\alpha^{-1}, \rho)}{P(\zeta\overline{\alpha}, \rho)}\right), \quad G_1(\zeta, \alpha) \equiv -\frac{\mathrm{i}}{2\pi} \log\left(\frac{|\alpha| P(\zeta\alpha^{-1}, \rho)}{P(\zeta\overline{\alpha}\rho^{-2}, \rho)}\right), \tag{7}$$

and where

$$W_U(\zeta, t) = I_+(\zeta, t) - I_-(\zeta, t), \tag{8}$$

with

$$\left.\begin{aligned} I_+(\zeta, t) &\equiv \frac{1}{2\pi} \oint_{|\zeta'|=1} \frac{\mathrm{d}\zeta'}{\zeta'} K(\zeta/\zeta', \rho(t)) \mathrm{Re}[-\mathrm{i}Uz(\zeta', t)], \\ I_-(\zeta, t) &\equiv \frac{1}{2\pi} \oint_{|\zeta'|=\rho(t)} \frac{\mathrm{d}\zeta'}{\zeta'} K(\zeta/\zeta', \rho(t)) \{\mathrm{Re}[\mathrm{i}Uz(\zeta', t)] + d_1(t)\}, \end{aligned}\right\} \tag{9}$$

and

$$d_1(t) = \frac{1}{2\pi\mathrm{i}} \left(\oint_{|\zeta|=1} \frac{\mathrm{d}\zeta}{\zeta} \mathrm{Re}[-\mathrm{i}Uz(\zeta, t)] - \oint_{|\zeta|=\rho(t)} \frac{\mathrm{d}\zeta}{\zeta} \mathrm{Re}[\mathrm{i}Uz(\zeta, t)] \right). \tag{10}$$

The function $K(\zeta, \rho)$ is related to $P(\zeta, \rho)$ by

$$K(\zeta, \rho) \equiv \frac{\zeta \partial P(\zeta, \rho)/\partial\zeta}{P(\zeta, \rho)}. \tag{11}$$

The first two terms in (6) produce the required circulations around the two wings (see, for example, Crowdy 2006, 2009); the term $W_U(\zeta, t)$ is associated with the fact that the two wings are in motion (see Crowdy, Surana & Yick 2007).

4.1. *A model system*

The solution is now complete. To illustrate how the results might be used, we now compute a natural (albeit physically unrealistic) extension of Lighthill's inviscid flow model. We ignore any effects of vortex shedding at the sharp edges of each plate, take Lighthill's value $\Gamma = 0.69$ and assume that it does not change as the wings separate. In reality, a Kutta condition will always be satisfied at the trailing edges of the wings so, given that Γ is fixed, we determine U dynamically by imposing this Kutta condition (by the geometrical symmetry, this is a single constraint). This is an artificial choice (and is the opposite of what usually happens in standard aerofoil theory) but it is consistent with our assumption that Γ remains fixed in time with no vortex shedding at the trailing edge. (In reality, U might depend on physiological factors associated with the organism.) To impose this choice, the two values (ζ_1 and ζ_2, say) on the unit circle $|\zeta| = 1$ given by the two conditions

$$\frac{\partial z(\zeta_1, t)}{\partial\zeta} = \frac{\partial z(\zeta_2, t)}{\partial\zeta} = 0 \tag{12}$$

are found using Newton's method. These are the preimages of the leading and trailing edges of the leftmost wing. If ζ_1 is the preimage of the trailing edge then U is determined by ensuring that the condition $\partial W(\zeta_1, t)/\partial\zeta = 0$ is satisfied (the condition is linear in U). A graph of U, as a function of s, is shown in figure 2 (from this

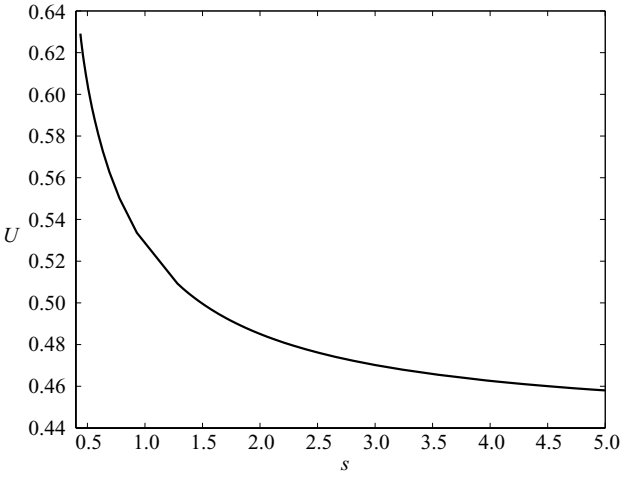

FIGURE 2. Graph, as a function of s, of the speed U of separation of the wings as given by imposing the Kutta condition at the trailing edges.

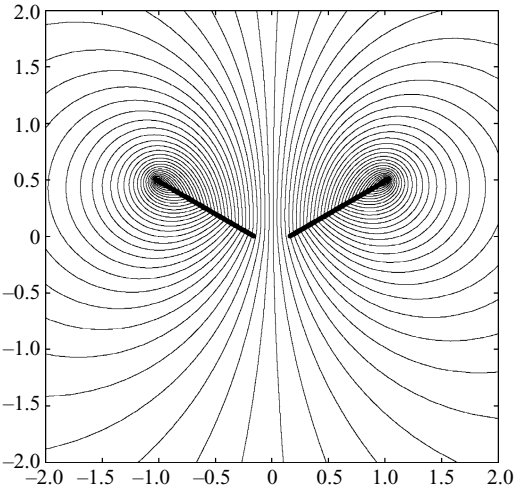

FIGURE 3. Instantaneous streamlines for a typical configuration of two separating wings showing the jet through the gap between them.

graph one could, if required, determine $s(t)$ as a function of time). If a single isolated wing had the same circulation around it, U would be given by the constant value (3); the fact that U is not constant is associated with the unsteady interference effects between the two wing sections. It is clear that unsteady interaction between the wings generally leads to increase in the velocity at which the wings must travel to satisfy the Kutta condition at the trailing edges. Within this model, the closer the wings are, the faster they must separate.

Figure 3 shows the streamlines, in a fixed frame, associated with a typical wing configuration during the opening phase. The jet flow through the gap between the wings is clearly visible. It is the momentum of this jet flow that balances the motion of the two wings.

5. Unsteady lift

By Bernouilli's theorem for unsteady irrotational flow (Acheson 1992), the fluid pressure is

$$p = -\left.\frac{\partial \phi}{\partial t}\right|_z - \frac{1}{2}|\boldsymbol{u}|^2 + H(t), \tag{13}$$

where $H(t)$ is some time-dependent function. Using the fact that

$$\phi = \mathrm{Re}[W(\zeta, t)], \quad |\boldsymbol{u}|^2 = \left|\frac{\partial W/\partial \zeta}{\partial z/\partial \zeta}\right|^2, \tag{14}$$

we can compute the total hydrodynamic force on each wing. It is given by

$$-\int p\boldsymbol{n}\,\mathrm{d}s, \tag{15}$$

where the integral is taken around each wing, $\boldsymbol{n} = (n_x, n_y)$ is the outward normal vector and $\mathrm{d}s$ is an element of arclength. In complex notation, the (complex) force on the leftmost wing becomes

$$F_x - \mathrm{i}F_y = \mathrm{i}\oint_{|\zeta|=1} \left(\left.\frac{\partial \phi}{\partial t}\right|_z + \frac{1}{2}\left|\frac{\partial W/\partial \zeta}{\partial z/\partial \zeta}\right|^2\right) \mathrm{d}\bar{z}. \tag{16}$$

Note that

$$\left.\frac{\partial \phi}{\partial t}\right|_z = \mathrm{Re}\left[\left.\frac{\partial W}{\partial t}\right|_z\right] \quad \text{and} \quad \left.\frac{\partial W}{\partial t}\right|_z = \left.\frac{\partial W}{\partial t}\right|_\zeta - \left(\frac{\partial W/\partial \zeta}{\partial z/\partial \zeta}\right)\left.\frac{\partial z}{\partial t}\right|_\zeta, \tag{17}$$

and these relations must be used to compute the integral in (16). The second integral in (17) has a simple pole singularity on the contour at the point ζ_2 (the preimage of the leading edge) and this is computed using the Plemelj formula for Cauchy-type integrals.

Figure 4 shows a graph of the lift development on the leftmost wing as a function of s. The initial separation between the two trailing edges of the wings is taken to be 10^{-2}. As $s \to \infty$, so that the wings are far apart, interference effects become negligible and the lift tends to the Kutta–Joukowski lift associated with an isolated wing in steady motion (with U and Γ related by (3)). It is also confirmed that the drag on the wings tends to zero. Out of interest, the instantaneous values of ΓU are superposed on this graph for comparison (by a dotted line): ΓU is the Kutta–Joukowski lift value for a single wing. It is interesting that the computed lift values for the two wings as they separate remain very close to ΓU under evolution and only depart appreciably from it when the plates are very close together. Unfortunately, this observation does not obviate the need to solve the full two-wing interaction problem to compute the lift because, as already observed, U is not constant but depends strongly on unsteady interaction effects.

The above calculations explore one scenario. The same mathematical approach can easily be adapted to study other situations.

6. Engineering applications

Inspired by Lighthill's analysis (Lighthill 1973), Furber & Ffowcs Williams (1979) proposed a design for an axial-flow compressor based on increasing the unsteady interaction effects between a moving (rotor) blade and a stationary (stator) blade due

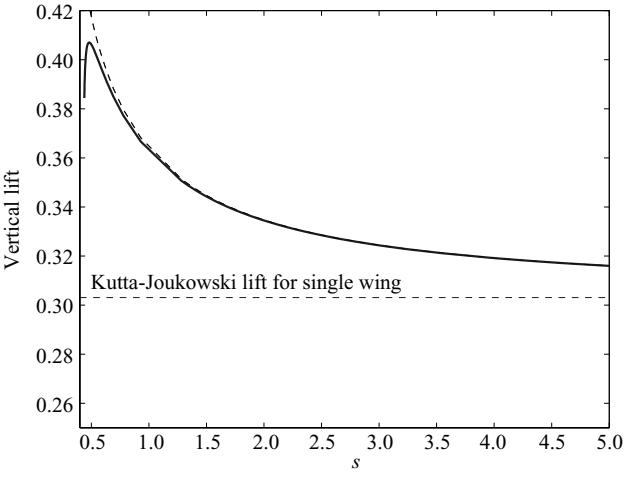

FIGURE 4. Unsteady lift development as a function of s. The instantaneous values of ΓU are superposed (dotted line). As $s \to \infty$, the lift tends to the Kutta–Joukowski lift for a single wing in steady motion.

to the Weis-Fogh mechanism. They performed potential flow calculations, following Lighthill (1973), for the phase in the cycle where the rotor and stator are in contact (the fluid domain is then simply connected). They find that a higher stage loading could be achieved under a wide range of operating conditions indicating significant performance advantages. Concerning an analysis of the full problem they state: 'Unfortunately we have found no way of obtaining an exact solution to the problem when the bodies are not in contact'. We now derive such a solution.

Both before and after the rotor touches down on the stator the fluid domain is doubly connected. Adapting, again, the results of Crowdy & Marshall (2006), the map $z(\zeta, t)$ from some annulus $\rho(t) < |\zeta| < 1$ to the fluid domain both before and after touchdown is

$$z(\zeta, t) = A(t) \left(\frac{P(\zeta e^{i\phi}, \rho(t)) P(\zeta e^{i\phi}, \rho(t))}{P(\zeta/\beta(t), \rho(t)) P(\zeta\beta(t), \rho(t))} \right) + d(t). \tag{18}$$

Here, $A(t)$, $\beta(t)$, $\rho(t)$ and $d(t)$ are the real functions of time and ϕ is the fixed angle between the rotor and stator. Equation (18) can be derived using similar considerations to those in the Appendix. Figure 5 shows the image of the circles $|\zeta| = \rho(t)$ and 1 under the map (18) for $\phi = \pi/4$ (before touchdown) and $\phi = -3\pi/4$ (after touchdown) and the appropriate values of the other parameters for a range of values of $s(t)$ (defined in figure 5). Note that $A(t)$, $\beta(t)$ and $\rho(t)$ can be determined once $s(t)$ is specified. Here, both plates have unit length (other choices are possible). Armed with $z(\zeta, t)$, the solution to the complex potential $W(\zeta, t)$ has the same general form (6) as in the Lighthill problem. The solution is then complete. As done earlier, the hydrodynamic forces on the plates throughout the cycle can now be readily computed. Again, it would be important to include the effects of shed vorticity in modelling this system but this might be done, following Edwards & Cheng (1982), using the Brown–Michael single-vortex model (see also Michelin & Llewellyn Smith 2009).

Finally, because both flow situations considered in this article involve doubly connected domains, it is possible, in principle, to translate all the analyses here into the language of elliptic function theory (although we make no claim that this is a

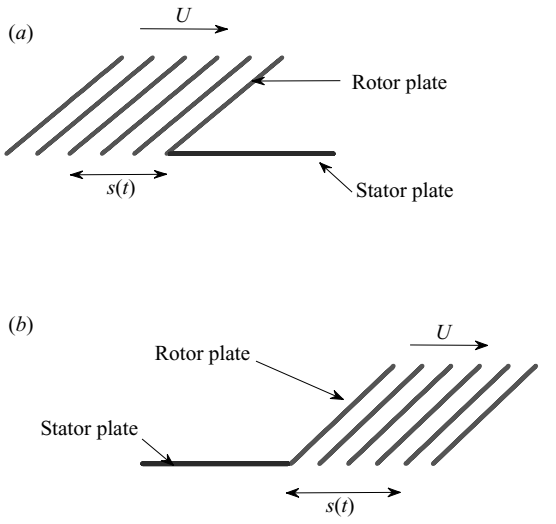

FIGURE 5. Image of the two circles $|\zeta| = \rho(t)$ and 1 under the conformal map (18) for $\phi = \pi/4$ (a) and $\phi = -3\pi/4$ (b) for six different values of $s(t)$ (from which the values of $A(t)$, $\rho(t)$ and $\mathrm{d}(t)$ follow on the imposition of the required geometrical constraints). The images are relevant to a rotor plate before and after it is in contact with a stator plate. All plates have unit length.

straightforward matter). However, if there is more than one rotor blade, then the fluid domain becomes triply connected (for two rotors blades) or higher connected (for three or more rotor blades) and elliptic function theory is irrelevant; nevertheless, the general calculus presented by Crowdy (2009), and used here, can still be applied in such situations (together with results on multiply connected slit mappings or Schwarz–Christoffel maps).

7. Discussion

While it is known that additional physical effects are crucial to the mechanism, our intention here has been to reappraise Lighthill's original analysis of the Weis-Fogh process in light of new theoretical developments for analysing ideal flows in multiply connected domains. We have, in a sense, completed Lighthill's solution and used it to compute the lift development in the spreading phase of his model. As for the leading-edge singularity, Edwards & Cheng (1982) have used a single-vortex model to study shedding from this edge during the opening phase (their analysis relied heavily on Lighthill's analytical solution (Lighthill 1973)). In principle, a similar analysis can now be performed during the separation phase with the help of the results herein.

This work has presented analytical solutions to two ideal flow problems involving doubly connected flow regions. The same methods are adaptable to the study of other flow problems involving two interacting flat plates. The formulae for the conformal maps found here may also be applied in a formulation of the Weis-Fogh mechanism at zero Reynolds number (Stokes flow) where complex variable techniques can also be used.

The author acknowledges the hospitality of the California Institute of Technology, where he was a Visiting Professor while this work was carried out. He also acknowledges support from an EPSRC Advanced Research Fellowship.

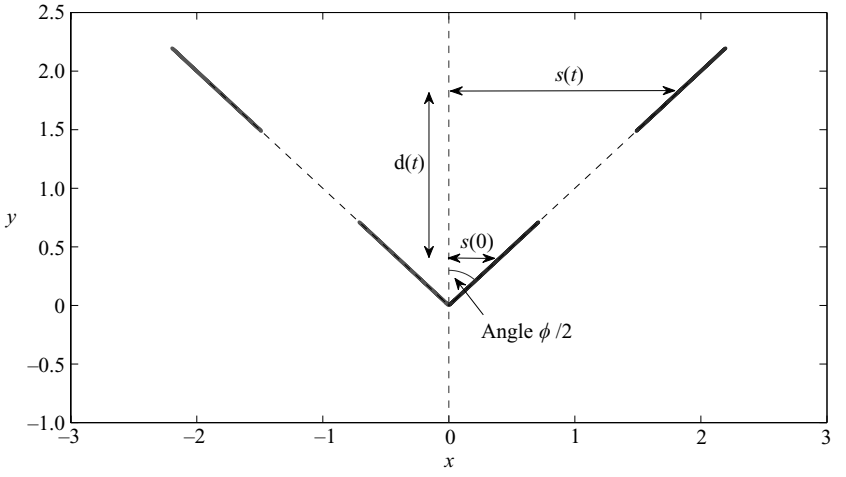

FIGURE 6. Image of the annulus $\rho(t) < |\zeta| < 1$ under $R(\zeta, t)$ for two different values of $\rho(t)$ (with $A(t)$ chosen so that all slits have unit length).

Appendix. The conformal mapping (4)

To understand (4), consider the image of $\rho(t) < |\zeta| < 1$ under the map

$$R(\zeta, t) = A(t)\left(\frac{P(\zeta\sqrt{\rho(t)}^{-1}\mathrm{e}^{\mathrm{i}\phi}, \rho(t))P(\zeta\sqrt{\rho(t)}\mathrm{e}^{\mathrm{i}\phi}, \rho(t))}{P(\zeta\sqrt{\rho(t)}^{-1}, \rho(t))P(\zeta\sqrt{\rho(t)}, \rho(t))}\right), \tag{19}$$

where $A(t)$ and $\rho(t)$ are some real parameters (to be determined). This is a doubly connected case of a so-called *radial slit map* as discussed by Crowdy & Marshall (2006) ($P(\zeta, \rho)$ is the *Schottky–Klein prime function* for this case—it is related to the first Jacobi theta function). It takes $|\zeta| = 1$ to a slit segment along the ray $\arg[R] = \phi$; it takes $|\zeta| = \rho(t)$ to a slit segment of the *same* length along the ray $\arg[R] = 0$. The rescaling parameter A is chosen so that each plate has unit length. Then, the distance $m(t) = s(t)/\sin(\phi/2)$ of the midpoint of each wing along the rays $\arg[R] = \phi$ and $\arg[R] = 0$ is controlled by choosing $\rho(t)$ appropriately (a simple Newton method can be used to find $\rho(t)$). Next, by multiplying $R(\zeta, t)$ by $\mathrm{i}\,\mathrm{e}^{-\mathrm{i}\phi/2}$ the two wings appear as in figure 6, which shows the images of $|\zeta| = 1, \rho(t)$ for two different $\rho(t)$-values. Simple geometrical considerations give

$$\mathrm{d}(t) = \cot(\phi/2)[s(t) - s(0)], \tag{20}$$

which must be subtracted from $\mathrm{i}\,\mathrm{e}^{-\mathrm{i}\phi/2}R(\zeta, t)$ so that the midpoints of the wings are at the same vertical position for different $s(t)$. The final result is $z(\zeta, t)$ in (4).

REFERENCES

ACHESON, D. J. 1992 *Elementary Fluid Dynamics*. Oxford University Press.

CROWDY, D. G. 2006 Calculating the lift on a finite stack of cylindrical aerofoils. *Proc. Roy. Soc.* A **462**, 1387–1407.

CROWDY, D. 2009 A new calculus for two-dimensional vortex dynamics. *Theor. Comput. Fluid Dyn.* (to appear).

CROWDY, D. G. & MARSHALL, J. S. 2006 Conformal mappings between canonical multiply connected domains. *Comput. Methods Funct. Theor.* **6** (1), 59–76.

CROWDY, D. G., SURANA, A. & YICK, K.-Y. 2007 The irrotational flow generated by two planar stirrers in inviscid fluid. *Phys. Fluids* **19**, 018103.

Edwards, R. H. & Cheng, H. K. 1982 The separation vortex in the Weis-Fogh circulation-generation mechanism. *J. Fluid Mech.* **120**, 463–473.

Furber, S. B. & Ffowcs Williams, J. E. 1979 Is the Weis-Fogh exploitable in turbomachinery? *J. Fluid Mech.* **94**, 519–540.

Lighthill, M. J. 1973 On the Weis-Fogh mechanism of lift generation. *J. Fluid Mech.* **60**, 1–17.

Mao, S. & Xin, Y. U. 2003 Flows around two airfoils performing fling and subsequent translation and subsequent clap. *Acta. Mech. Sinica* **19** (2), 103–117.

Maxworthy, T. 1979 Experiments on the Weis-Fogh mechanism of lift generation by insects in hovering flight. Part A. Dynamics of the 'fling'. *J. Fluid Mech.* **93**, 47–63.

Michelin, S. & Llewellyn Smith, S. G. 2009 Falling cards and flapping flags: understanding fluid–solid interactions using an unsteady point vortex model. *Theor. Comput. Fluid Dyn.* (In press).

Spedding, G. R. & Maxworthy, T. 1986 The generation of circulation and lift in a rigid two-dimensional fling. *J. Fluid Mech.* **165**, 247–272.

Weis-Fogh, T. 1973 Quick estimates of flight fitness in hovering animals, including novel mechanisms for lift production. *J. Exp. Biol.* **59**, 169–230.